Original Research Article: full paper

(2022), «EUREKA: Physics and Engineering»
Number 3

DESIGN AND PRACTICE OF SIMPLE FIRST-ORDER ALL-PASS FILTERS USING COMMERCIALLY AVAILABLE IC AND THEIR APPLICATIONS

Atirarj Suksawad
Department of Electronics and Telecommunication Engineering[1]

Angkana Charoenmee
Department of Electronics and Telecommunication Engineering[1]

Suphaphorn Panikhom
Department of Electronics and Telecommunication Engineering[1]

Khunpan Patimaprakorn
Department of Electrical Engineering[1]

Adirek Jantakun✉
Department of Electronics and Telecommunication Engineering[1]
adirek.ja@rmuti.ac.th

[1]*Rajamangala University of Technology Isan*
150 Srichan Road Muang, Khon Kaen, Thailand, 40000

✉**Corresponding author**

Abstract

First-order all-pass filter circuits, both non-inverting and inverting, could be the focus of this article, which could include the design and implementation of first-order all-pass filter circuits. Using a standard integrated circuit (IC): AD830, as well as a single resistor and a single capacitor, the proposed first-order all-pass filters could well be built. The AD830 is an integrated circuit (IC) manufactured by Analog Devices Corporation that is available for purchase. The pole frequency and phase response of the proposed all-pass filters could well be directly modified by attuning the resistor in the circuit. Aside from that, the output voltage has a low impedance, making it appropriate for use in voltage-mode circuits. In addition, the proposed first-order all-pass filter is used to design the multiphase sinusoidal oscillator, which serves as an example of an application wherein the oscillation condition can be adjusted without impacting the frequency. The gain and phase responses of the proposed all-pass filters, as well as their phase response adjustment, time-domain response, and total harmonic distortion of signals, are all shown via computer simulation using the PSPICE software, as well as their experimental results. For the proposed circuits, a statistical analysis is coupled with a Monte Carlo simulation to estimate the performance of the circuits. In accordance with the results of this study, a theoretical design suitable for developing a worksheet for teaching and learning in electrical and electronic engineering laboratories has already been developed.

Keywords: low-output-impedance, high-input-impedance, non-inverting, inverting, first-order, all-pass filter, multiphase sinusoidal oscillator, frequency of oscillation, oscillation condition, difference amplifier.

DOI: 10.21303/2461-4262.2022.002416

1. Introduction

An all-pass filter is used to convert an input signal to a constant amplitude output signal at all frequencies. The phase of the output signal, on the other hand, will be shifted relative to the frequency of the input signal. Several publications on the implementation of the all-pass filter (APF) circuits have appeared in the last few years [1–29]. With this feature, the APF circuit is then applicable to a variety of applications such as phase shifters [1–29], single phase oscillator [1], quadrature oscillators [1–9], multiphase oscillators 1, [10–13], and high-Q band-pass filters [14]. The voltage-mode first-order all-pass filters have been presented in the literature, using a variety of active building blocks. They are constructed with active elements such as current feedback operational amplifiers (CFOAs) [1, 13], current controlled conveyors (CCCII) [2, 14, 20], LT1228 [3], second-genera-

tion current conveyors (CCII) [4, 8, 26], differential voltage current conveyors (DVCC) [5, 12, 22], voltage differencing inverting buffered amplifier (VDIBA) [6], differential voltage current conveyor transconductance amplifier (DVCCTA) [7], fully differential second generation current conveyors (FDCCII) [9–10], operational transresistance amplifier (OTRA) [11], a fully balanced voltage differencing buffered amplifier (FB-VDBA) [15], current controlled conveyor transconductance amplifier (CCCTA) [16], operational transconductance amplifiers (OTAs) [17, 18, 21], voltage differencing transconductance amplifier (VDTA) [19], current controlled third-generation voltage conveyor (CC-VCIII–) [23], controlled current conveyor transconductance amplifier (MO-CCCCTA) [24], current-controlled current differencing buffered amplifier (CCCDBA) [25], Current controlled current conveyor transconductance amplifier (CCCCTA) [27], differential difference current conveyor transconductance amplifier (DDCCTA) [28], and current differencing buffer amplifier (CDBA) [29]. Most APF circuits can be adjusted for the pole frequency and phase response by electronic adjustment [4–6, 10–12, 25, 27, 28]. The APF presents the output port at a low-impedance [1, 4–6, 9–13, 15, 25, 27] or provides both inverting and non-inverting outputs [1, 7, 13, 26]. Furthermore, the advantage of a single active element of APF [3] is that it can be easily constructed and implemented in experiments. A review of the literature on reported voltage-mode APFs reveals the following weaknesses:

– they have a high output impedance [2–4, 6–8, 11, 14, 16–19, 21–24, 26, 28, 29] that cannot be directly cascaded to load or next stages, which require the use of a voltage buffer for cascading;

– they cannot be implemented from a commercially available IC [2, 4–7, 9–12, 14, 16–19, 21–25, 27–29] that has not been experimentally tested;

– they require matching conditions [1, 2, 4, 7–10, 13–16, 19, 22, 24–26, 29] that are inconvenienced for operation;

– they need an active building block which contains multiple current output terminals [6, 19] used in producing integrated circuits with high cost.

A summary and comparison of the previous publications and researches in the literatures [1–29] can be reported in **Table 1**.

The purpose of this article is to present a design idea for all-pass filters based on the commercially available IC:AD830. Both the non-inverting and inverting first-order all-pass filters have low output impedance as well as have no need for the constraint matching condition of active or passive elements. A non-inverting all-pass filter is applied to a multiphase oscillator as a sample. To confirm the performance of the first-order all-pass filter and a multiphase oscillator circuit is shown with PSPICE simulation and experimental results according to the theories.

Table 1

The summary and comparison of previous all-pass filters

Ref.	Type of Active Building Block	Commercially Available IC	Type of APF	High I/P	Low O/P	Require extension of port/ terminal	Require matching condition	Application	Verification
1	**2**	**3**	**4**	**5**	**6**	**7**	**8**	**9**	**10**
1	CFOA	Yes (2 AD844)	Both	✓	✓	×	✓	Osc.	Sim./Exp.
2	CCCII	No	Non-inverting	×	×	×	✓	Osc.	Sim.
3	LT1228	Yes (1 LT1228)	Non-inverting	×	×	×	×	Osc.	Sim.
4	CCII	Yes (1 AD844)	Non-inverting	×	×	×	✓	Osc.	Sim./Exp.
5	DDCC	No	Inverting	×	✓	×	×	Osc.	Sim.
6	VDIBA	Yes (2 OPA860)	Both	×	×	×	×	Osc.	Sim./Exp.
7	DVCCTA	No	Non-inverting	✓	×	✓	✓	Osc.	Sim.
8	CCII	Yes (2 AD844)	Non-inverting	✓	×	×	✓	Osc.	Exp.
9	FDCCII	No	Non-inverting	✓	✓	✓	✓	Osc.	Sim.
10	FDCCII	No	Inverting	✓	✓	✓	×	Osc.	Sim.

Continuation of the Table 1

1	2	3	4	5	6	7	8	9	10
11	OTRA	No	Inverting	×	×	×	×	Osc.	Sim.
12	DDCC	No	Non-inverting	✓	✓	×	×	Osc.	Sim.
13	CFOA	Yes (2 AD844)	Both	✓	✓	×	✓	Osc.	Sim./Exp.
14	CCCII	No	Non-inverting	×	×	×	✓	High-Q	Sim.
15	FB-VDBA	Yes (1 MAX435, 1 OPA860)	Inverting	✓	✓	✓	✓	×	Exp.
16	CCCTA	No.	Non-inverting	×	×	×	✓	×	Sim.
17	OTA	No	Non-inverting	×	×	×	×	×	Sim.
18	OTA	No	Inverting	✓	×	×	×	×	Sim.
19	VDTA	No	Non-inverting	×	×	✓	✓	×	Sim.
20	CCCII+OP	Yes (1 OPA860, 1 AD8130)	Inverting	✓	✓	×	×	×	Sim./Exp.
21	OTA	No	Both	✓	×	✓	×	×	Sim.
22	VDCC	No	Inverting	×	×	×	✓	×	Sim.
23	CC-VCIII	No	Inverting	×	×	×	×	×	Sim.
24	MO-CCCCTA	No	Non-inverting	✓	×	✓	✓	×	Sim.
25	CDBA	No	Non-inverting	×	✓	×	✓	×	Sim.
26	CCII	Yes (1 AD844)	Inverting	×	×	×	✓	×	Sim.
27	CCCCTA	No	Non-inverting	✓	×	✓	×	×	Sim.
28	DDCCTA	No	Non-inverting	×	×	×	×	×	Sim.
29	CDBA	No	Non-inverting	×	×	×	✓	×	Sim.
Prop. APFs **Fig. 4, *a***	AD830	Yes (2 AD830)	Non-inverting	✓	✓	×	×	×	×
Fig. 4, *b*	AD830	Yes (1 AD830)	Non-inverting	×	✓	×	×	Oscillator	Sim./Exp.
Fig. 6, *a*	AD830	Yes (2 AD830)	Inverting	✓	✓	×	×	×	×
Fig. 6, *b*	AD830	Yes (1 AD830)	Inverting	×	✓	×	×	×	Sim./Exp.

Remarks : Sim. = Simulation, Exp. = Experiment

2. Materials and methods

2. 1. The details of AD830

The AD830 is a difference amplifier in an 8-pin package produced for commercially available by Analog Devices Corporation [30]. **Fig. 1** shows the electrical symbol, and pin configuration of AD830. The input voltages (pin 1, 2, 3 and 4) of the AD830 are high-impedances and the output voltage (pin 7) is low-impedance. The supply voltage of AD830 can be operated from ±5 V to ±15 V. The following mathematical function can be used to describe the electrical characteristics of the AD830:

$$V_X = A_O\left[\left(V_{Y1} - V_{Y2}\right) + \left(V_{Y3} - V_{Y4}\right)\right]. \quad (1)$$

$A_o \cong \infty$ is the voltage gain in the open loop.

Fig. 2 demonstrates how easily the AD830 may be set up to create the difference between three signals, V_{Y1}, V_{Y2}, and V_{Y3}, in which the applied differential signal is precisely replicated at the output. The voltage output of the circuit in **Fig. 2** can be written as:

$$V_{out} = V_{Y1} - V_{Y2} + V_{Y3}. \quad (2)$$

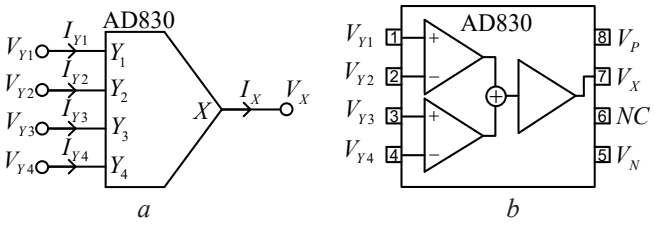

Fig. 1. AD830 [30]: *a* – Electrical symbol; *b* – Pin configuration

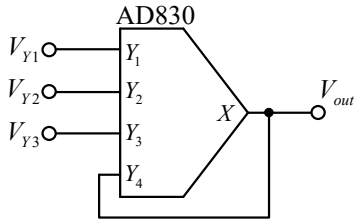

Fig. 2. AD830 as a Difference Amplifier

2. 2. Concept voltage-mode first-order all-pass filters

2. 2. 1. Non-inverting first-order all-pass filters

The method for synthesizing all-pass filters as presented in **Fig. 3** is a conceptual design of the non-inverting first-order all-pass filter (APF+) on a circuit block diagram that consists of the first-order high-pass filter, the amplifier at defined $k_1 = 2$, and the summing. The circuit of the proposed non-inverting APF is schematically designed as in **Fig. 4, *a*** and **Fig. 4, *b***.

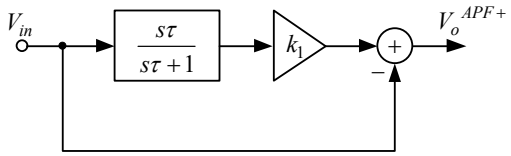

Fig. 3. Conceptual design of the non-inverting first-order APF

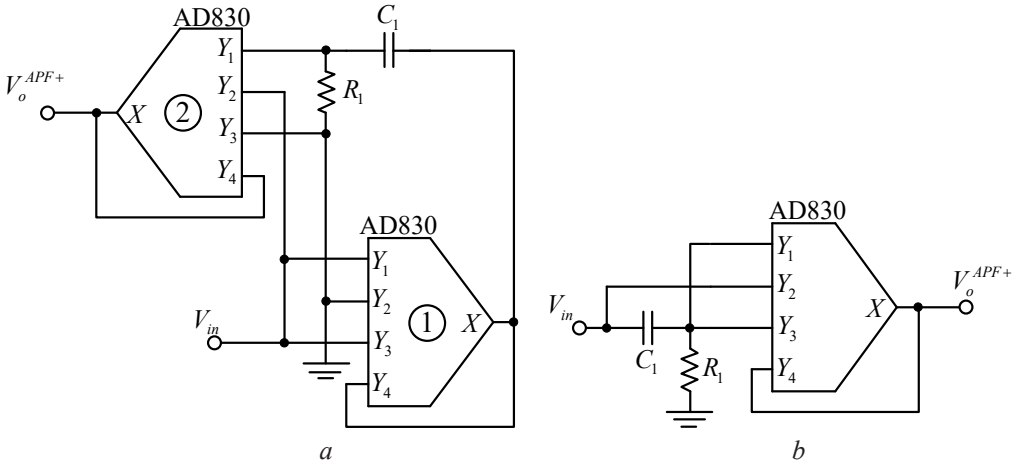

Fig. 4. The proposed non-inverting all-pass filter: *a* – Two AD803; *b* – Single AD830

The proposed non-inverting APF is shown in **Fig. 4**, where ***a*** uses a single capacitor, a single resistor, and two AD830s, where the first AD830 acts as an amplifier of the input signal (k_1) at high-input-impedance without resistors. The second AD830 connects a capacitor and a resistor as a first-order high-pass filter and sums the input signal, with the output voltage of the circuit being low-impedance. Additionally, the proposed non-inverting APF is shown in **Fig. 4**,

where ***b*** is simply designed with a single AD830, a single capacitor, and a single resistor. **Fig. 4, *b***, shows the AD830 connected to a capacitor and a resistor to create a high-pass filter. It can be seen that the AD830 in **Fig. 4, *b*** can function as both an amplifier and a summing amplifier. Furthermore, the voltage output port of the circuit is low-impedance, so it can be conveniently cascaded or connected to other stages or circuits. The electrical properties of AD830 in equation (2) of the circuits in **Fig. 4, *a*, *b*** can be analyzed and presented by the voltage transfer function of the proposed APF circuit as follows:

$$\frac{V_o^{APF+}}{V_{in}} = \frac{sC_1R_1 - 1}{sC_1R_1 + 1}. \tag{3}$$

The pole frequency and voltage gain of the proposed non-inverting APF are the same that can be analyzed in equations (4), (5), respectively.

$$\omega_p = \frac{1}{C_1R_1}, \tag{4}$$

$$\phi(\omega) = 180 - 2\tan^{-1}(\omega C_1R_1). \tag{5}$$

The voltage gain of the proposed non-inverting APF can be analyzed and written as:

$$G(\omega) = \left|\frac{V_o^{APF+}}{V_{in}}\right| = 1. \tag{6}$$

According to equation (6), the input and output voltages are equal. From equations (4), (5), the adjustment of the pole frequency and the phase response can be controlled via R_1 and C_1.

2. 2. 2. Inverting first-order all-pass filters

Fig. 5 shows the design concept of the inverting first-order all-pass filter (APF–) that consists of a first-order low-pass filter, an amplifier defined as $k_2 = 2$, and summing. From this concept, the circuit in **Fig. 6, *a*** is then designed with two AD830s, a single capacitor, and a single resistor. The first AD830 is an amplifier of the input signal (k_2). The second AD830 connects a capacitor and a resistor to be the low-pass filter and sums the signal from pin Y_2. This design is for high-input-impedance and low-output-impedance. The inverting APF in **Fig. 6, *b*** is designed with only a single AD830, a single capacitor, and a single resistor. The output port of the inverting APF is low-impedance. This design can reduce the amount of equipment required from the circuit in **Fig. 6, *a***.

The voltage transfer function of the proposed inverting APF circuit in **Fig. 6, *a*, *b*** is written as follows:

$$\frac{V_o^{APF-}}{V_{in}} = \frac{1 - sC_1R_1}{1 + sC_1R_1}. \tag{7}$$

From equation (7), the pole frequency, voltage gain, and phase response of the proposed inverting APF can be given as:

$$\omega_p = \frac{1}{C_1R_1}, \tag{8}$$

$$\phi(\omega) = -2\tan^{-1}(\omega C_1R_1), \tag{9}$$

and

$$G(\omega) = \left|\frac{V_0^{APF-}}{V_{in}}\right| = 1. \tag{10}$$

From equation (10), the input and output voltages are equal. The pole frequency and phase response can be modified with equations (8), (9), respectively, by adjusting R_1 and C_1.

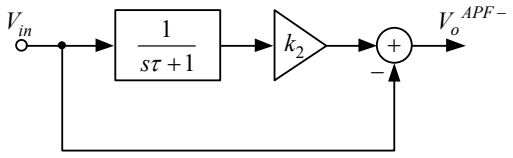

(V_{o3})

Fig. 5. Conceptual design of the inverting first-order APF

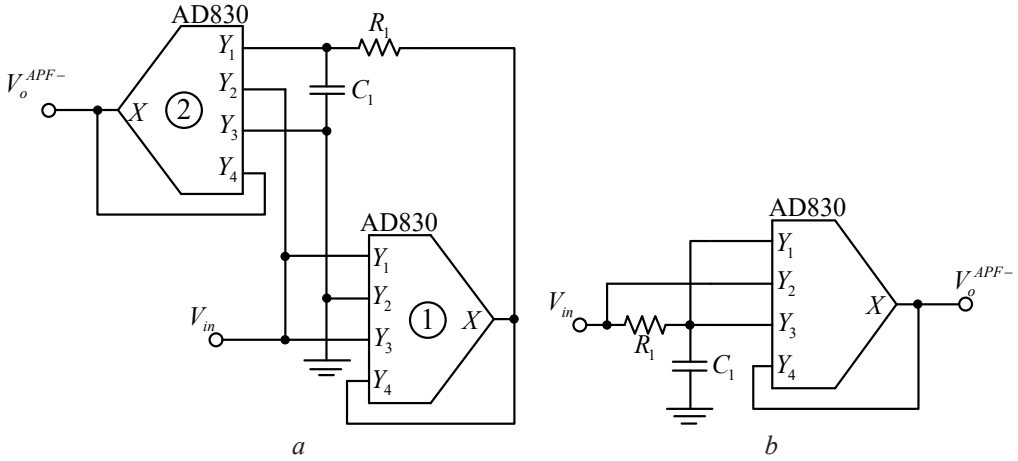

a *b*

Fig. 6. The proposed inverting all-pass filter: *a* – Two AD803; *b* – Single AD830

The non-ideal of the voltage in practice is partly caused by parasitic components. They can be found at the input ports and output port of the AD830. The high-impedance ports are the Y_1, Y_2, Y_3, and Y_4 ports. These parasitic elements of the ports have resistors and capacitors connected to the ground as well as the output port X and they are in a series of resistors with low-parasitic values. **Fig. 7** shows the details of the parasitic elements. It can be described as follows.

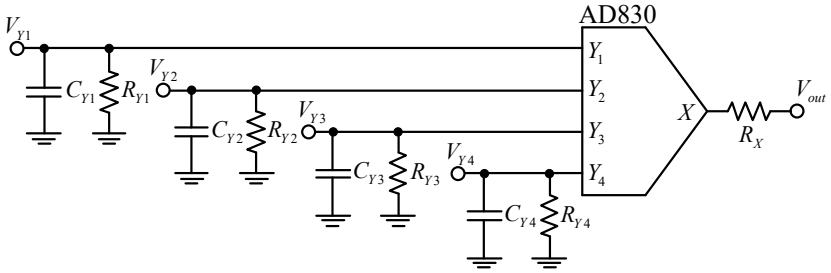

Fig. 7. AD830 with the parasitic elements

2. 2. 3. Non-ideal study of non-inverting APF

The parasitic elements of AD830 are included in the characteristic equation of the proposed non-inverting APF in **Fig. 4, *b***. Thus, the new features when $R_1 \gg R_X$ were studied and analyzed as follows:

$$\frac{V_o^{APF+}}{V_{in}} = \frac{s(C_1 + C_T) - G_T}{s(C_1 + C_T) + G_T}. \tag{11}$$

The pole frequency and phase response of non-inverting APF circuits are modified to (12), (13), respectively.

$$\omega_p = \frac{G_T}{C_1 + C_T}, \tag{12}$$

and

$$\phi = 180 - 2\tan^{-1}\left(\frac{C_1 + C_T}{G_T}\right), \tag{13}$$

where

$$G_T = \frac{1}{R_1} + \frac{1}{R_{Y1}} + \frac{1}{R_{Y3}} \text{ and } C_T = C_{Y1} + C_{Y3}.$$

2. 2. 4. Non-ideal study of inverting APF

The non-ideal study of AD830 are incorporated into the characteristic equation of the proposed inverting APF in **Fig. 6, *b***. As a result, the new transfer functions at $R_1 \gg R_X$ were analyzed as follows:

$$\frac{V_o{}^{APF-}}{V_{in}} = \frac{(G_1 - G_T) + sC_T}{(G_1 + G_T) + sC_T}. \tag{14}$$

From equation (14), the pole frequency and phase response of inverting APF circuits are modified as

$$\omega_p = \frac{G_1 + G_T}{C_T}, \tag{15}$$

and

$$\phi = -2\tan^{-1}\frac{C_T}{G_1 + G_T}, \tag{16}$$

where

$$G_T = \frac{1}{R_{Y1}} + \frac{1}{R_{Y3}},\ G_1 = \frac{1}{R_1},$$

and

$$C_T = C_1 + C_{Y1} + C_{Y3}.$$

Parasitic elements have an effect on the performance of the proposed non-inverting APF and inverting APF. The impact of the pole frequency and phase response is caused by equations (12), (13), (15), and (16), which can be resolved by slightly adjusting the resistance. The multiphase sinusoidal oscillator (MSO) is an example of the application of the proposed APF. The MSO is designed by cascading three proposed non-inverting APFs and positioning them in a feedback loop to show an application example in **Fig. 8**. The output voltage at the low-impedance of the MSO is at nodes V_{o1}, V_{o2}, and V_{o3}. It can be cascaded or connected to other stages or circuits without the need for a voltage buffer. The system loop gain of the proposed MSO can be written as follows:

$$LG(\mathrm{s}) = K\left(\frac{sC_1R_1 - 1}{sC_1R_1 + 1}\right)^n. \tag{17}$$

The phase of the system loop gain can be expressed in equation (18).

$$\angle H(\mathrm{s}) = 2n\phi = 2n\left(-2\tan^{-1}\left(\omega C_1R_1\right)\right) = -2\pi. \tag{18}$$

Equation (17) can be used when n is an odd number. The output signals have a phase of 360/n, which is in accordance with equation (18). An oscillator circuit can generate sinusoidal signals if the oscillation requirement is achieved, as in:

$$K = \frac{R_{G2}}{R_{G1}} + 1 \geq 1. \tag{19}$$

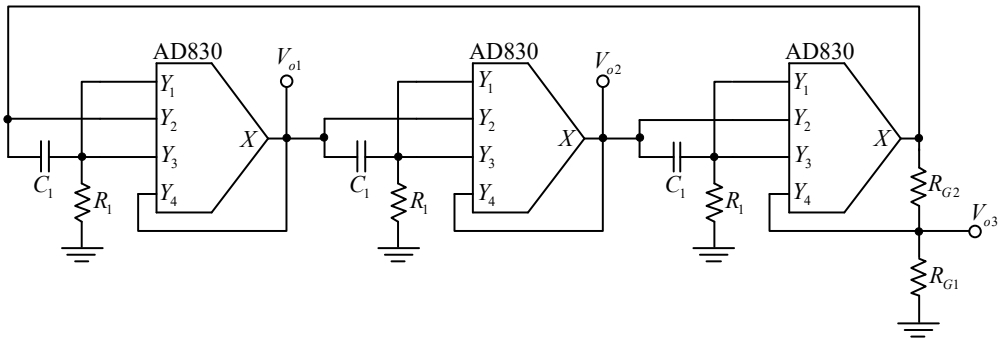

Fig. 8. Multiphase sinusoidal oscillator

The frequency of oscillation (FO) is given by:

$$\omega_{osc} = \frac{1}{C_1 R_1} \tan \frac{\pi}{6} . \quad (20)$$

As can be observed in equations (19), (20), by adjusting K, the oscillation condition can be easily changed without affecting the frequency. Also, the frequency of oscillation can be adjusted by C_1 and R_1.

3. Results and discussion

A simulation of the proposed first-order all-pass filters used sample circuits as in **Fig. 4, *b*; 6, *b*** by verifying the circuit performance and theoretical validity using the PSPICE program. To simulate, the AD830 macro-model was adopted. Both proposed APFs used passive elements with values of $R_1 = 1$ kΩ and $C_1 = 1$ nF. The supply voltage chosen for use was ±5 V.

Fig. 9, *a*, *b* show the gain and phase responses of the non-inverting and inverting APFs, respectively, when compared to a theoretical model. The simulation results represent the phase response from 180° to 0° of the non-inverting APF and the phase response from 0° to 180° of the inverting APF. The voltage gain of both APFs was approximately 0 dB. The pole frequencies of the non-inverting APF and the inverting APF were about 157 kHz and 156 kHz, respectively. When calculated using equations (4), (8), it deviated from the theoretical figure by about 1.35 % and 1.97 %. Thus, it will be seen that the simulation results were greater compared to the theoretical analysis.

The results in **Fig. 10, *a*, *b*** followed adjustments in the phase response of the non-inverting APF in **Fig. 4, *b*** and the inverting APF in **Fig. 6, *b*** which adjusted the value of R_1 in both circuits to 250 Ω, 500 Ω, 1 kΩ, and 2 kΩ, respectively. The phase responses at 90° of the non-inverting APF were transformed to 79.04 kHz, 157.73 kHz, 314.25 kHz, and 623.93 kHz, respectively, with the inverting APF transformed to 79.43, 159.56, 316.22, and 630.54 kHz, respectively. The results agreed with the theoretical analysis when equations (4), (8) were compared.

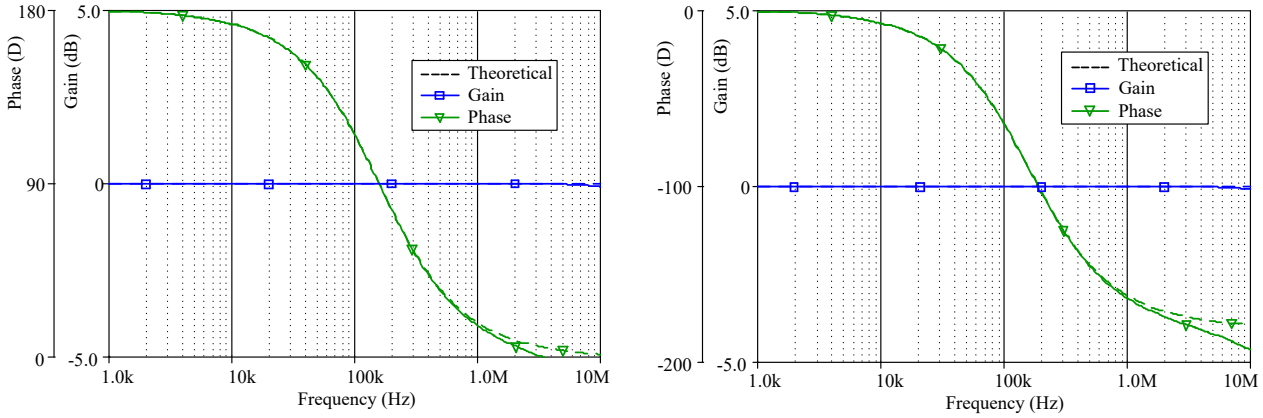

Fig. 9. Gain and phase responses of the proposed APF: *a* – APF+; *b* – APF–

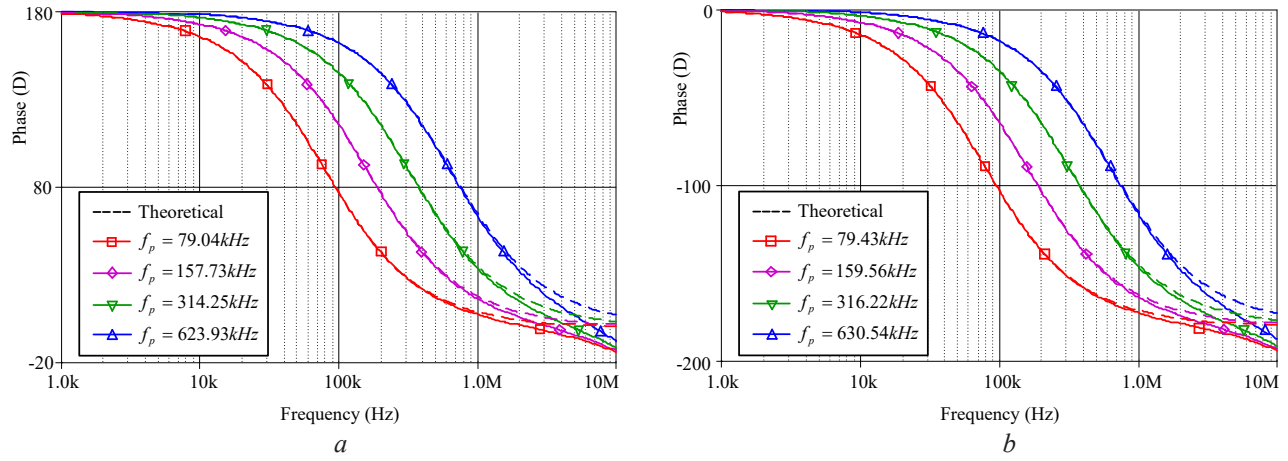

Fig. 10. Phase response for different values of R_1: *a* – APF+; *b* – APF–

The Monte Carlo (MC) method was utilized to examine the tolerance error of the passive device since this has an effect on the proposed APF. The MC was set to a Gaussian distribution for 100 samples, and the tolerance errors of the resistor and the capacitor were 1 % and 10 %. The MC analysis of both the proposed APFs is illustrated in **Fig. 11, *a*** for the gain response of the non-inverting APF, in **Fig. 11, *b*** for the gain response of the inverting APF, **Fig. 11, *c*** for the phase response of the non-inverting APF, and **Fig. 11, *d*** for the phase response of the inverting APF.

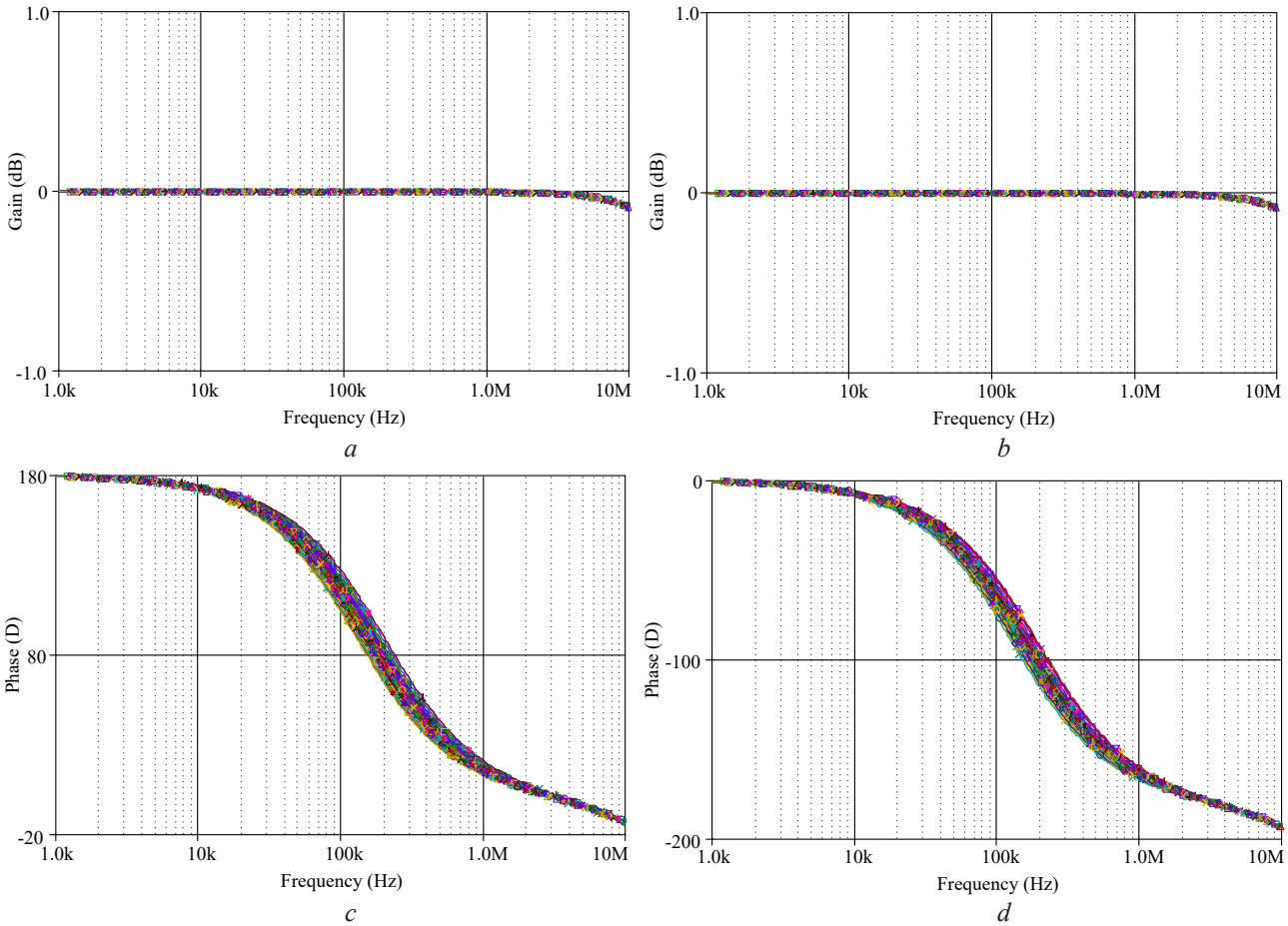

Fig. 11. The Monte Carlo analysis: *a* – Gain response of APF+; *b* – Gain response of APF–; *c* – Phase response of APF+; *d* – Phase response of APF–

The histogram of the gain and phase at frequency 159.15 kHz of both APFs is illustrated in **Fig. 12**, and **Table 2**. The non-inverting APF has a mean gain response of –0.0052 dB, a median of –0.0052 dB, and a standard deviation of 0.000087. The non-inverting APF has a mean phase response of 89.62°, a median of 88.53°, and a standard deviation of 5.84. The inverting APF has a mean gain response of –0.0048 dB, a median of –0.0048 dB, and a standard deviation of 0.000092. The inverting APF has a mean phase response of –90.57°, a median of –90.62°, and a standard deviation of 5.36.

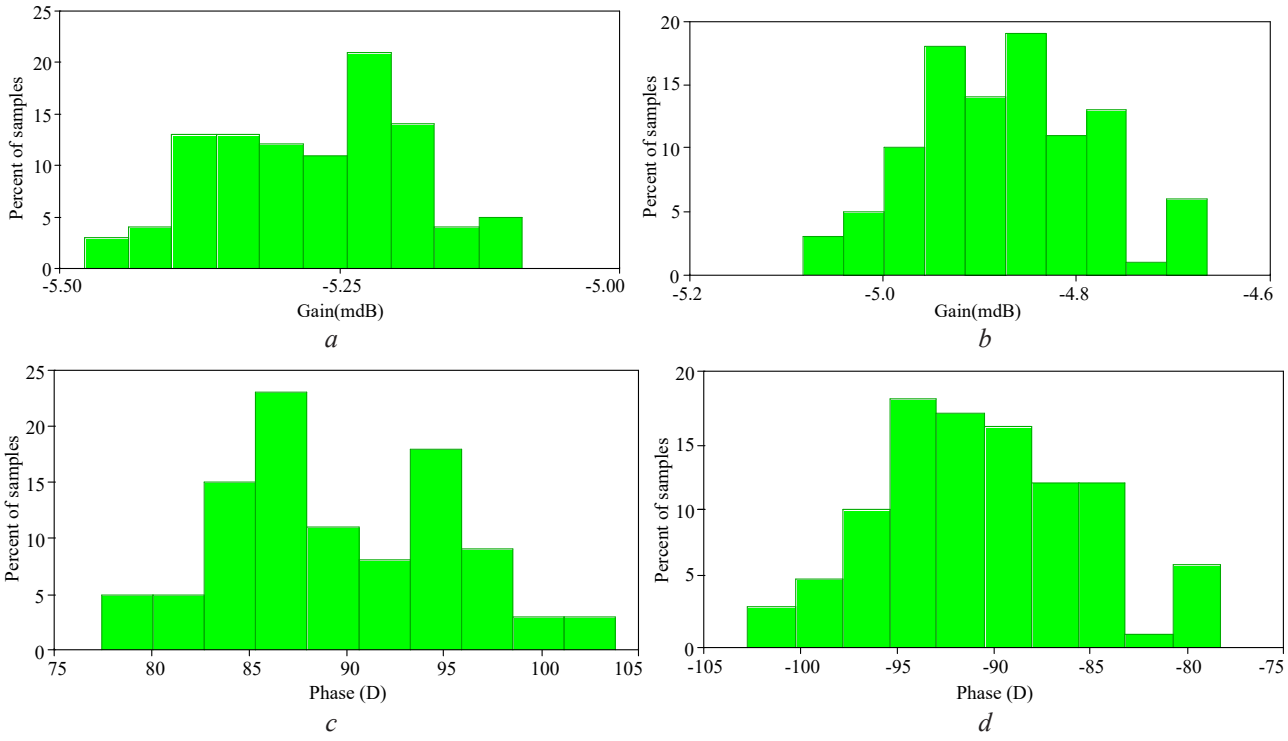

Fig. 12. Histograms of the proposed APF at frequency 159.15 kHz: *a* – Gain response of APF+; *b* – Gain response of APF–; *c* – Phase response of APF+; *d* – Phase response of APF–

Table 2
Statistical outputs of MC analysis

No.	APF	Response	Statistical components and their values			
			Number of simple	Mean	Median	Standard deviation
1	Non-inverting	Gain	100	–0.0052 dB	–0.0052 dB	0.000087
		Phase	100	89.62 Degree	88.53 Degree	5.84
2	Inverting	Gain	100	–0.0048 dB	–0.0048 dB	0.000092
		Phase	100	–90.57 Degree	–90.62 Degree	5.36

The total harmonic distortion (THD) of the output non-inverting APF and inverting APF in simulation is shown in **Fig. 13** when sweeping the input signal from 0.1 $V_{p\text{-}p}$ to 2 $V_{p\text{-}p}$. The percentage THD of both APFs was a minimum of 0.01 % and a maximum of 0.30 %.

The simulation results of the proposed multiphase sinusoidal oscillator were obtained using the circuit in **Fig. 8** by configuring the supply voltage of ±5 V, the passive elements as $R_1 = 470\ \Omega$ and $C_1 = 0.47$ nF. The MSO was able to generate sinusoidal signals when $K \geq 1$, $R_{G1} = 10\ \text{k}\Omega$ and $R_{G2} = 100\ \Omega$ were configured to conform to equation (19). **Fig. 14, *a*** shows the simulation of the initial state signals, and **Fig. 14, *b*** shows the steady-state signals of the sinusoidal output waveform. The output spectrum of multiphase signals in **Fig. 15** shows an output frequency of about 400.0 kHz, which deviated from 415.97 kHz by about 3.83 % from equation (20), and the total

harmonic distortion (THD) of V_{o1}, V_{o2}, and V_{o3} were about 3.41 %, 1.58 %, and 2.90 %, respectively. The simulation results were analyzed using the MC because the tolerance error of the passive device affected the MSO. The MC was set to a Gaussian distribution for 100 samples, and the tolerance errors of each resistor and capacitor were 1 % and 10 %, respectively. **Fig. 16, *a*, *b*** demonstrate the spread of the frequency domain and histograms of the output (V_{o1}). The mean, median, and standard deviation of the frequency oscillation were 410.87 kHz, 407.63 kHz, and 24.48 kHz, respectively.

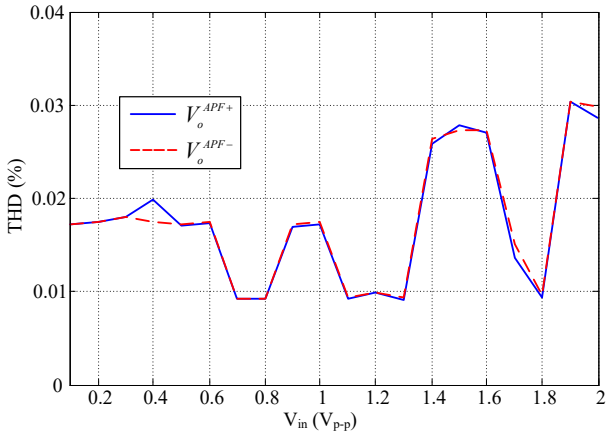

Fig. 13. %THD of the proposed APF

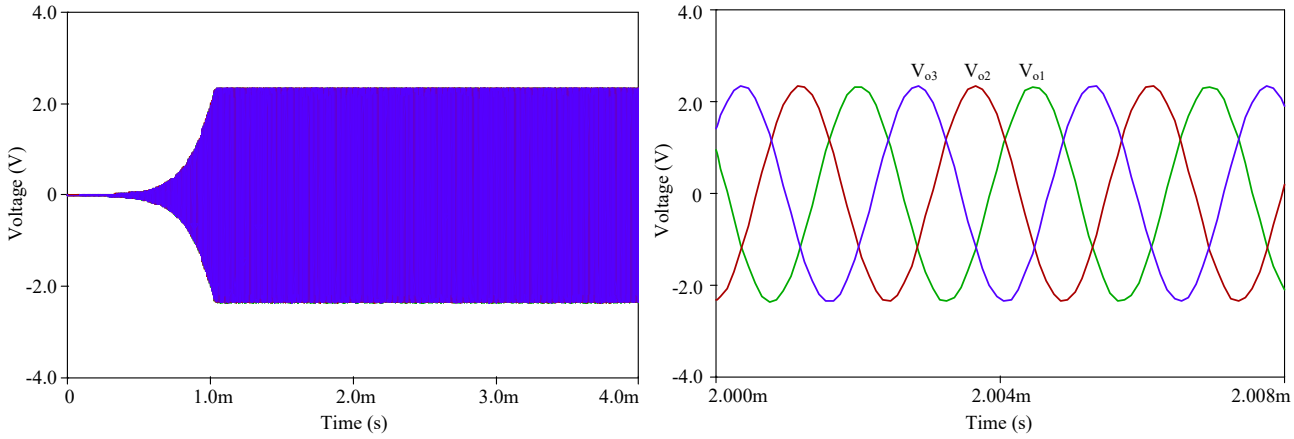

a *b*

Fig. 14. The simulation of output waveforms: *a* – Initial state signals; *b* – Steady state signals

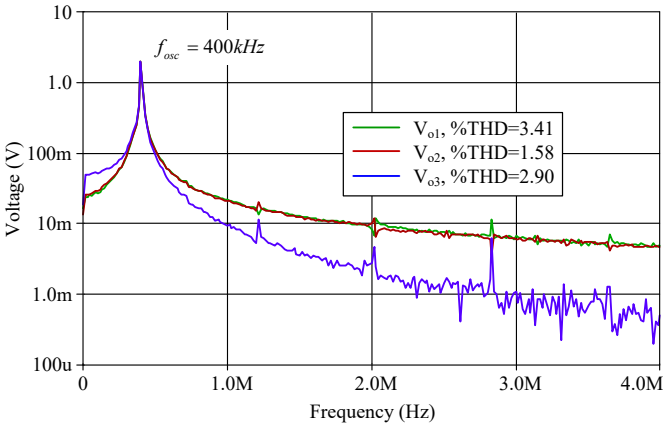

Fig. 15. Output spectrum of multiphase oscillator

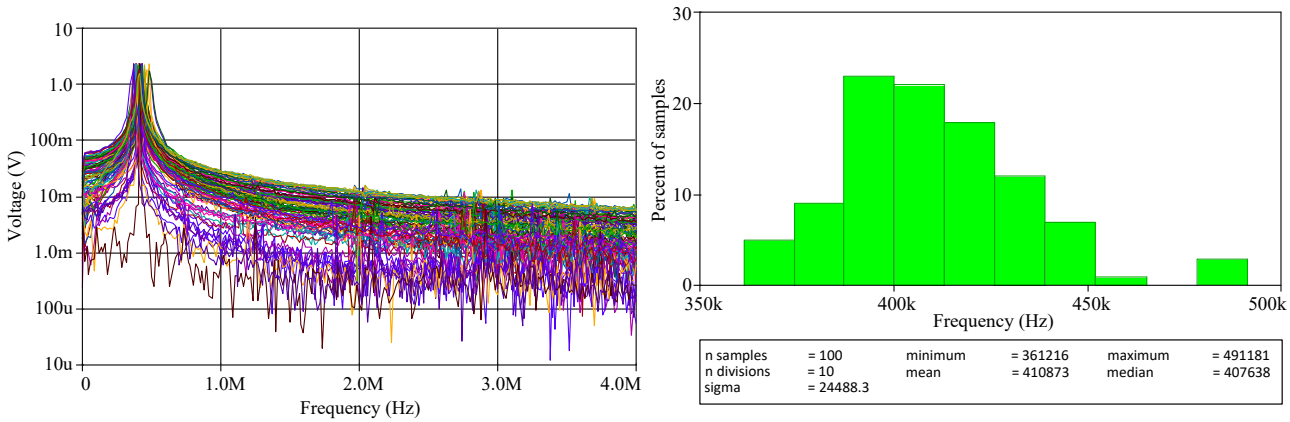

a *b*

Fig. 16. The Monte Carlo analysis of the oscillator:
a – the spread of the frequency domain of the V_{o1}; *b* – histograms of the FO at V_{o1}

To verify the circuit performance and theoretical validity of the proposed first-order all-pass filter circuit by the experimental non-inverting APF in **Fig. 4, *b*** and the inverting APF in **Fig. 6, *b***. The experiment was conducted by using the commercially available IC: AD830. The proposed APF in **Fig. 4, *b***; **6, *b*** was connected to a supply voltage of ±5 V by the Siglent SPD3303C power supply. The passive elements are chosen as $R_1 = 1$ kΩ and $C_1 = 1$ nF. The performance of the circuit was measured using a Keysight DSOX3024T oscilloscope. The frequency response analyzer was set at 200 m$V_{p\text{-}p}$ amplitude and sweep frequency from 1 kHz to 10 MHz.

The gain and phase responses of the non-inverting APF and the inverting APF are shown in **Fig. 17, *a*, *b***, respectively. It was found that the gain responses were about 0 dB for all frequencies of both APFs, which is consistent with the theoretical analysis results in equations (6) and (10). The phase responses of non-inverting APF varied from about 180° to –17°. The pole frequency was about 158.5 kHz with a 90° phase shift. The phase responses of the inverting APF ranged from approximately 0° to –195°. The pole frequency was about 154.88 kHz with a –90° phase shift. These results are consistent with equation (5) of the non-inverting APF and equation (9) of the inverting APF.

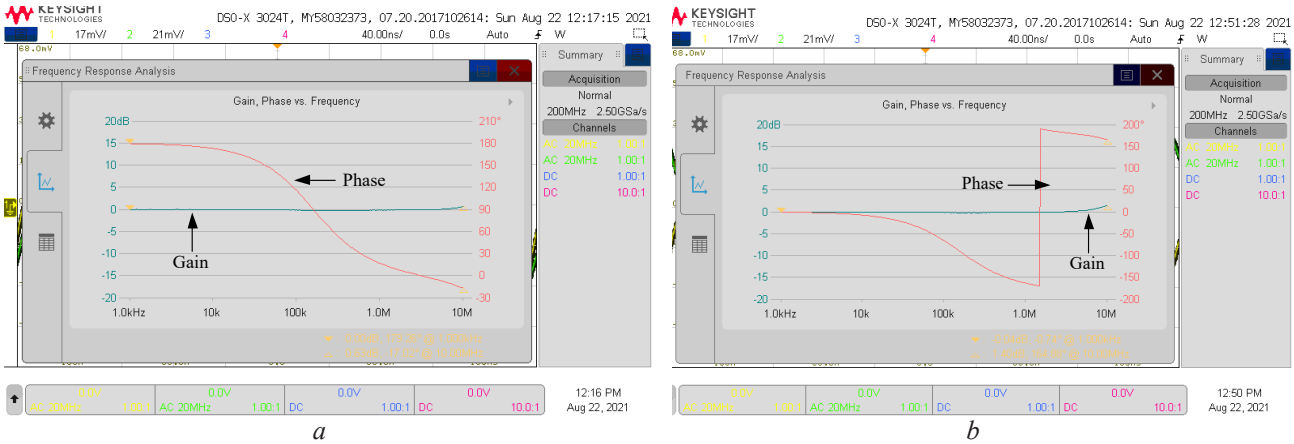

a *b*

Fig. 17. Gain and phase response of experimental results: *a* – APF+; *b* – APF–

Fig. 18, *a* shows the experimental results of output voltage in time-domain waveforms when the input voltage of the non-inverting APF is a sinusoidal signal with a frequency of 158.54 kHz and an amplitude of about 200 m$V_{p\text{-}p}$. These results are consistent with phase response and voltage gain in equations (5), (6). **Fig. 18, *b*** shows the gain and phase response of experimental results from inverting APF when the input has a frequency of 158.55 kHz and an amplitude of about 200 m$V_{p\text{-}p}$. The results correspond with the following equations (9), (10). The phase relationship between waveforms V_{in} and V_{out} of the non-inverting APF is about 90.06° at the frequency

of 158.4 kHz, and the phase relationship between waveforms V_{in} and V_{out} of the inverting APF is about 90° at the frequency of 158.55 kHz. Both results are shown in **Fig. 19, *a*, *b***, respectively, which agree with the theoretical analysis in phase response equation (5) of the non-inverting APF and phase response equation (9) of the inverting APF.

The results in **Fig. 20** demonstrate the adjustment in the phase response of non-inverting APF in **Fig. 4, *b*** by adjusting the value of R_1 to 500 Ω, 1 kΩ, and 2 kΩ, respectively. It is evident that the phase responses at 90° of the frequency transformed to 77.62 kHz, 158.48 kHz, and 309.02 kHz. The results of the phase responses agree with the theoretical analysis in equation (5).

The proposed multiphase sinusoidal oscillator in **Fig. 8** was set with a voltage supply at ±5 V. Moreover, passive components were defined using $C_1 = 0.47$ nF and $R_1 = 470$ Ω. When the oscillation condition was set as $R_{G1} = 10$ kΩ and $R_{G2} = 100$ Ω to define $K = 1.01$, which corresponds to the conditions in equation (19), then the circuit generated sinusoidal signals.

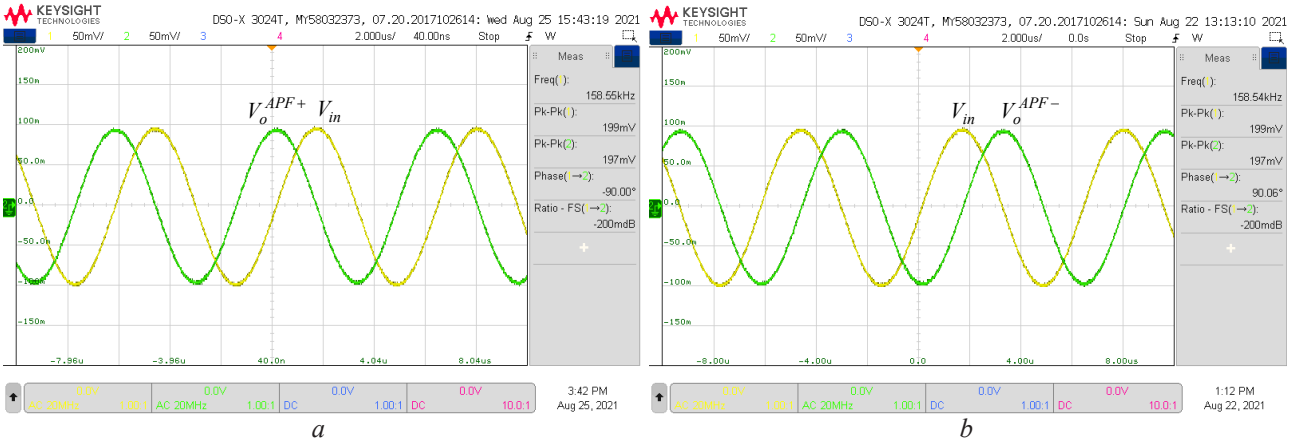

a *b*

Fig. 18. The time-domain response of APF: *a* – APF+; *b* – APF–

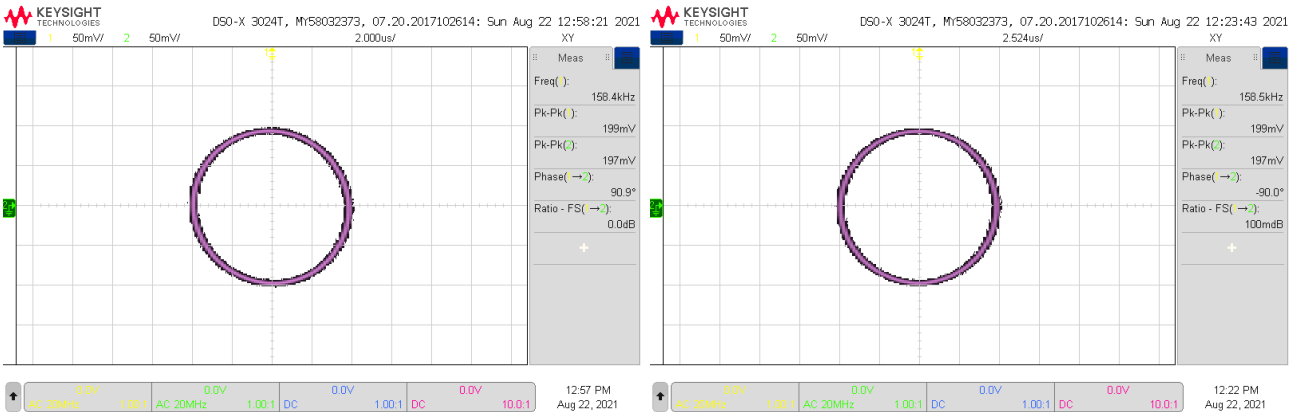

a *b*

Fig. 19. Lissajous figure of the sinusoidal waveforms: *a* – APF+; *b* – APF–

Fig. 21 shows the results of the multiphase sinusoidal waveforms. The oscillation frequency was 402.25 kHz, which inaccurate was about 3.29 % of the theoretical value of the equation (20). Additionally, the phase relationship between V_{o1}, V_{o2}, and V_{o3} output voltages was 119.20°, 120.90°, and 120.10°, respectively. This error may occur as a consequence of passive element tolerance issues. The tolerance errors of the MSO were about 3 % for three passive resistors and 30 % for three passive capacitors. However, the resulting frequency and phase of the MSO are still consistent with the theoretical.

The example relationship between the waveforms of the MSO in **Fig. 22** is about 120° at output V_{o1} and V_{o2} when measured by using the *XY*-mode which the result agrees with equation (18).

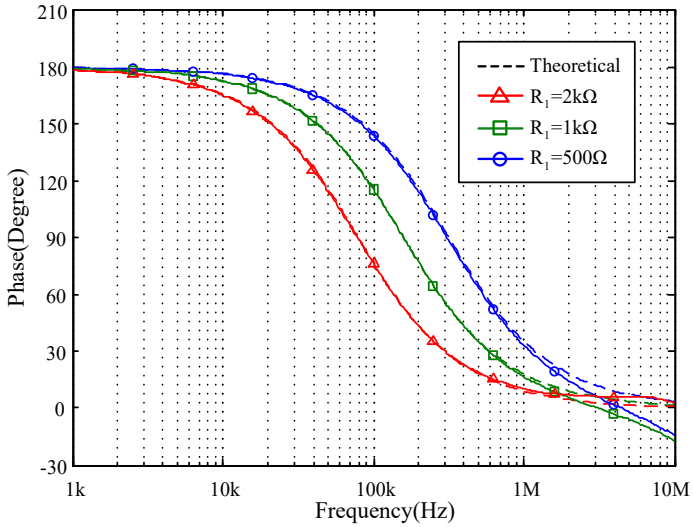

Fig. 20. Phase response of APF+ for different values of R_1

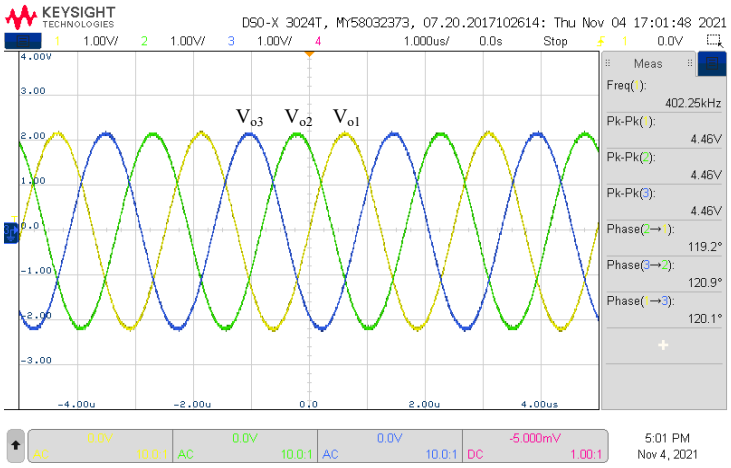

Fig. 21. The MSO output waveforms

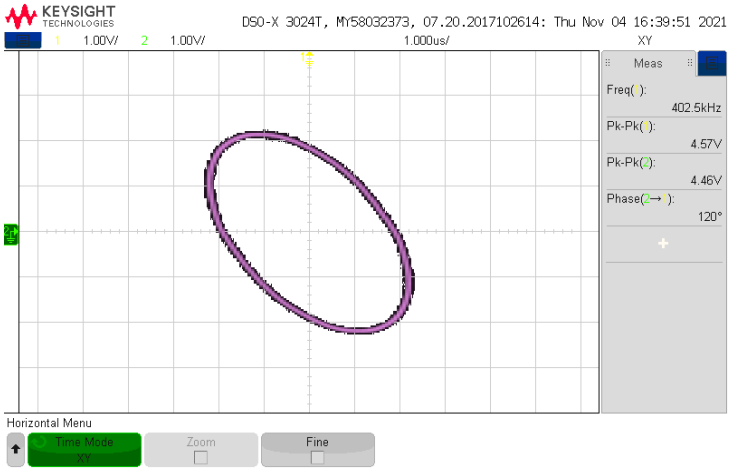

Fig. 22. Lissajous figure of sinusoidal MSO waveforms

The THD of the output voltage MSO (V_{o1}) in **Fig. 23, *a*** is approximately 0.240 %, and the amplitude of the other harmonic is 56.8 dB greater than the first harmonic. The THD of the output voltage MSO (V_{o2}) is about 0.351 %. As shown in **Fig. 23, *b***, the magnitude of the first to other

harmonic is 53.2 dB, while the THD of the output voltage MSO (V_{o3}) in **Fig. 23, *c*** is about 0.283 % and the magnitude of the first to other harmonic is 54.0 dB, respectively.

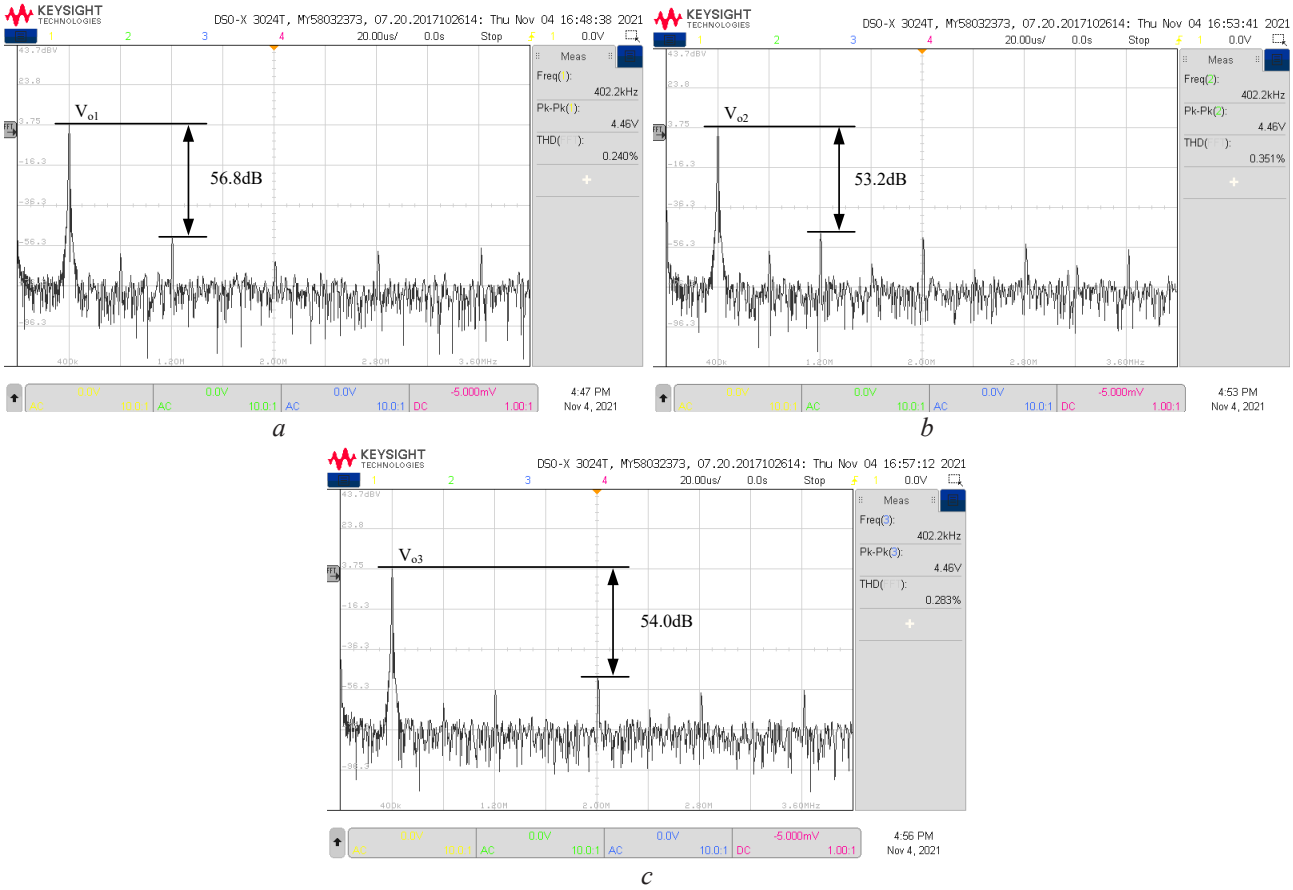

Fig. 23. The frequency spectrum of the output signals MSO:
a – The output (V_{o1}); *b* – The output (V_{o2}); *c* – The output (V_{o3})

It can be seen that a commercially available integrated circuit used in the proposed APFs makes lab tests simpler and cheaper. The pole frequency and phase response of non-inverting and inverting APFs are in line with the theoretical analysis and MC analysis as presented in **Table 2**. It is interesting that the proposed APFs are appropriately used in electrical and electronic engineering study. However, the proposed APFs are still limited because the AD830 can operate at a maximum frequency of about 10 MHz.

4. Conclusions

In the proposed non-inverting and inverting APF creation concepts, each kind of APF can be constructed with a commercial IC AD830, a single capacitor, and a single resistor. The APFs can adjust the phase response by adjusting the resistance. Additionally, the voltage output ports of both first-order APFs are low-impedance, so they can be cascaded or connected to other stages or circuits. The multiphase sinusoidal oscillator was used to prove the proposed non-inverting APF. The simulation and experimental results confirmed the performance of the circuit. Also, the results agree with the theoretical analysis. The experiment results can be described as an example that the non-inverting and inverting APF had a pole frequency of about 158.54 kHz and 158.55 kHz, respectively, which is an error of 0.383 % and 0.377 %, respectively. The adjustment of phase responses of 90° was experimentally demonstrated by changing resistors by 500 Ω, 1 kΩ, and 2 kΩ. After changing these, the pole frequencies were 77.62 kHz, 158.48 kHz, and 309.02 kHz, respectively. In applying APF, the multiphase sinusoidal oscillator can be generated an oscillation frequency of 402.25 kHz

with an error of 3.29 %. From these, the APFs then are appropriate for developing a worksheet for teaching and learning in electronic laboratories.

Acknowledgement

This research was supported by a grant from the Faculty of Engineering, Rajamangala University of Technology, Isan, Khon Kaen Campus, Khon Kaen, Thailand.

References

[1] Yuce, E., Verma, R., Pandey, N., Minaei, S. (2019). New CFOA-based first-order all-pass filters and their applications. AEU – International Journal of Electronics and Communications, 103, 57–63. doi: https://doi.org/10.1016/j.aeue.2019.02.017

[2] Maheshwari, S. (2004). New voltage and current-mode APS using current controlled conveyor. International Journal of Electronics, 91 (12), 735–743. doi: https://doi.org/10.1080/00207210412331332880

[3] Chaichana, A., Siripongdee, S., Jaikla, W. (2019). Electronically Adjustable Voltage-mode First-order Allpass Filter Using Single Commercially Available IC. IOP Conference Series: Materials Science and Engineering, 559 (1), 012009. doi: https://doi.org/10.1088/1757-899x/559/1/012009

[4] Yucel, F., Yuce, E. (2015). A new single CCII- based voltage-mode first-order all-pass filter and its quadrature oscillator application. Scientia Iranica, 22 (3), 1068–1076. Available at: http://scientiairanica.sharif.edu/article_3700.html

[5] Horng, J.-W., Hou, C.-L., Chang, C.-M., Lin, Y.-T., Shiu, I.-C., Chiu, W.-Y. (2006). First-order allpass filter and sinusoidal oscillators using DDCCs. International Journal of Electronics, 93 (7), 457–466. doi: https://doi.org/10.1080/00207210600711481

[6] Herencsar, N., Minaei, S., Koton, J., Yuce, E., Vrba, K. (2012). New resistorless and electronically tunable realization of dual-output VM all-pass filter using VDIBA. Analog Integrated Circuits and Signal Processing, 74 (1), 141–154. doi: https://doi.org/10.1007/s10470-012-9936-2

[7] Pandey, N., Pandey, R., Paul, S. K. (2012). A first order all pass filter and its application in a quadrature oscillator. Journal of Electron Devices, 12, 772–777. Available at: https://silo.tips/download/a-first-order-all-pass-filter-and-its-application-in-a-quadrature-oscillator

[8] Horng, J.-W. (2005). Current conveyors based allpass filters and quadrature oscillators employing grounded capacitors and resistors. Computers & Electrical Engineering, 31 (1), 81–92. doi: https://doi.org/10.1016/j.compeleceng.2004.11.006

[9] Mohan, J., Maheshwari, S., Chauhan, D. S. (2010). Voltage Mode Cascadable AllPass Sections Using Single Active Element and Grounded Passive Components. Circuits and Systems, 01 (01), 5–11. doi: https://doi.org/10.4236/cs.2010.11002

[10] Maheshwari, S., Mohan, J., Chauhan, D. S. (2010). Voltage-mode cascadable all-pass sections with two grounded passive components and one active element. IET Circuits, Devices & Systems, 4 (2), 113. doi: https://doi.org/10.1049/iet-cds.2009.0167

[11] Pandey, R., Pandey, N., Mullick, R., Yadav, S., Anurag, R. (2015). All Pass Network Based MSO Using OTRA. Advances in Electronics, 2015, 1–7. doi: https://doi.org/10.1155/2015/382360

[12] Chaturvedi, B., Maheshwari, S. (2012). An ideal voltage-mode all-pass filter and its application. Journal of Communication and Computer, 9, 613–623. Available at: https://www.researchgate.net/publication/237018593_An_ideal_voltage_mode_all-pass_filter_and_its_applications_JCC

[13] Senani, R., Bhaskar, D. R., Kumar, P. (2021). Two-CFOA-grounded-capacitor first-order all-pass filter configurations with ideally infinite input impedance. AEU – International Journal of Electronics and Communications, 137, 153742. doi: https://doi.org/10.1016/j.aeue.2021.153742

[14] Toker, A., Gune, E. O., Ozoguz, S. (2001). New high-Q band-pass filter configuration using current controlled current conveyor based all-pass filters. ICECS 2001. 8th IEEE International Conference on Electronics, Circuits and Systems (Cat. No. 01EX483). doi: https://doi.org/10.1109/icecs.2001.957706

[15] Biolek, D., Biolkova, V., Kolka, Z. (2010). All-Pass filter employing fully balanced voltage differencing buffered amplifier. IEEE Latin American Symposium on Circuits and Systems, 232–235. Available at: https://user.unob.cz/Biolek/veda/articles/LASCAS2010_1.pdf

[16] Tangsrirat, W., Pukkalanun, T., Surakampontorn, W. (2010). Resistorless realization of current-mode first-order allpass filter using current differencing transconductance amplifiers. Microelectronics Journal, 41 (2-3), 178–183. doi: https://doi.org/10.1016/j.mejo.2010.02.001

[17] Kumngern, M. (2012). Realization of electronically tunable first-order allpass filter using single-ended OTAs. 2012 IEEE Symposium on Industrial Electronics and Applications. doi: https://doi.org/10.1109/isiea.2012.6496607

[18] Kumngern, M., Chanwutitum, J. (2012). Voltage-mode first-order allpass filter using single-ended OTAs and grounded capacitor. 2012 Second International Conference on Digital Information and Communication Technology and It's Applications (DICTAP). doi: https://doi.org/10.1109/dictap.2012.6215363

[19] Maneewan, S., Udorn, N., Silapan, P., Duangmalai, D., Jaikla, W. (2014). A Voltage-Mode First Order Allpass Filter Based on VDTA. Advances in Electrical and Electronic Engineering, 12 (1). doi: https://doi.org/10.15598/aeee.v12i1.846

[20] Bajer, J., Biolek, D. (2010). Voltage-mode electronically tunable all-pass filter employing CCCII+, One capacitor and differential-input voltage buffer. 2010 IEEE 26-Th Convention of Electrical and Electronics Engineers in Israel. doi: https://doi.org/10.1109/eeei.2010.5661939

[21] Tsukutani, T., Tsunetsugu, H., Sumi, Y., Yabuki, N. (2010). Electronically tunable first-order all pass sections using OTAs. 2010 International Conference on Computer Applications and Industrial Electronics. doi: https://doi.org/10.1109/iccaie.2010.5735141

[22] Uttaphut, P. (2019). Voltage-Mode First-Order Allpass Filter with Grounded Capacitor and Electronic Controllability. PRZEGLĄD ELEKTROTECHNICZNY, 1 (3), 103–106. doi: https://doi.org/10.15199/48.2019.03.24

[23] Herencsar, N., Koton, J., Vrba, K., Metin, B. (2011). Novel voltage conveyor with electronic tuning and its application to resistorless all-pass filter. 2011 34th International Conference on Telecommunications and Signal Processing (TSP). doi: https://doi.org/10.1109/tsp.2011.6043729

[24] Pandey, N., Arora, P., Kapur, S., Malhotra, S. (2011). First order voltage mode MO-CCCCTA based all pass filter. 2011 International Conference on Communications and Signal Processing. doi: https://doi.org/10.1109/iccsp.2011.5739380

[25] Maheshwari, S. (2007). Voltage-Mode All-Pass Filters Including Minimum Component Count Circuits. Active and Passive Electronic Components, 2007, 1–5. doi: https://doi.org/10.1155/2007/79159

[26] Shah, N. A., Rather, M. F. (2006). Realization of voltage-mode CCII-based all pass filter and its inverse version. Indian Journal of Pure and Applied Physics, 44, 269–271.

[27] Janda, T., Onsa-ard, W., Jantakun, A. (2018). The Realization of Four-mode First-order Allpass Filter Based-on CCCCTAs. Proceedings of the 10th International Conference on Sciences, Technology and Innovation for Sustainable Well-Being (STISWB 2018).

[28] Kumngern, M., Mongkol, V., Junnapiya, S. (2013). Voltage-mode allpass section employing only one DDCCTA and one capacitor. 2013 Eleventh International Conference on ICT and Knowledge Engineering. doi: https://doi.org/10.1109/ictke.2013.6756279

[29] Kaçar, F., Özcelep, Y. (2011). CDBA Based Voltage-Mode First-Order All-pass Filter Topologies. IU-Journal of Electrical & Electronics Engineering, 11 (1), 1327–1332. Available at: https://dergipark.org.tr/en/download/article-file/99242

[30] High speed, video difference amplifier. Data Sheet AD830. Available at: https://www.analog.com/media/en/technical-documentation/data-sheets/AD830.pdf

Received date 16.12.2021
Accepted date 02.05.2022
Published date 31.05.2022

How to cite: *Suksawad, A., Charoenmee, A., Panikhom, S., Patimaprakorn, K., Jantakun, A. (2022). Design and practice of simple first-order all-pass filters using commercially available IC and their applications. EUREKA: Physics and Engineering, 3, 40–56. doi: https://doi.org/10.21303/2461-4262.2022.002416*